

Na₂₃K₉Tl_{15.3}: An Unusual Zintl Compound Containing Apparent Tl₅⁷⁻, Tl₄⁸⁻, Tl₃⁷⁻, and Tl⁵⁻ Anions

Zhen-Chao Dong and John D. Corbett*

Ames Laboratory—DOE¹ and Department of Chemistry, Iowa State University, Ames, Iowa 50011

Received January 5, 1996[⊗]

Reaction of the neat elements in tantalum containers at 400 °C and then 150 °C gives the pure title phase. X-ray crystallography shows that the hexagonal structure (*P6₃/mmc*, *Z* = 2, *a* = 11.235(1) Å, *b* = 30.133(5) Å) contains relatively high symmetry clusters Tl₅⁷⁻ (*D_{3h}*), Tl₄⁸⁻ (*C_{3v}*, *~ T_d*), and the new Tl₃⁷⁻ (*D_{∞h}*) plus Tl⁵⁻, the last two disordered over the same elongated site in 1:2 proportions. Cation solvation of these anions is tight and specific, providing good Coulombic trapping of weakly bound electrons on the isolated cluster anions. The observed disorder makes the compound structurally a Zintl phase with a closed shell electron count. EHMO calculations on the novel Tl₃⁷⁻ reveal some bonding similarities with the isoelectronic CO₂, with two good σ(*s,p*) bonding and two weakly bonding π MO's. The Tl–Tl bond lengths therein (3.14 Å) are evidently consistent with multiple bonding. The weak temperature-independent paramagnetism and metallic conductivity (*ρ*₂₉₃ ~ 90 μΩ·cm) of the phase are discussed.

Introduction

Classical Zintl compounds are characterized by both the electron transfer from the electropositive to the electronegative atoms (ionic part) and the formation of simple anions or anionic substructures with apparent *octet* configurations (covalent part).^{2,3} Extension of the concept to include polyanions with *delocalized* but still *closed-shell* bonding allows one to correlate structures with electron counts (e.g., Wade's rules) in a broader range of systems.^{3–7} A large number of binary and ternary compounds between alkali or alkaline-earth (*s*-block) metals and the later main-group (*p*-block) elements have been characterized and almost without exception shown to meet Zintl criteria structurally.³ The electron-poorer examples, the triels (Tr = Al, Ga, In, Tl) in particular, are especially interesting because their compounds are expected to probe the limits of the Zintl concept and applicability.^{3,7,8} The variety of polyanionic species observed in alkali-metal–thallium systems gives tremendous testimony to the applicability of simple electron counting rules, to the versatility possible in structures, and to the importance of suitable cavities for the cations. For example, ATl (*A* = Li, Na, K, Cs) phases exhibit a structural trend from LiTl (CsCl-type) through the classic NaTl (stuffed diamond) to the related KTl and CsTl with isolated compressed octahedra, all of which relate to the efficient packing of A⁺ and (Tl⁻)_{*n*} over a widely varying range of A⁺ sizes.⁹ Similarly, mixed-cation compounds with increased size and packing flexibilities have been shown

to yield novel thallium clusters such as Tl₅⁷⁻ and Tl₉⁹⁻ in Na₂K₂₁Tl₁₉,¹⁰ Tl₁₃¹¹⁻ in Na₃K₈Tl₁₃,¹¹ and Tl₁₂M¹²⁻ in Na₁₄K₆Tl₁₈M (*M* = Mg, Zn–Hg).¹² The occurrence of diverse thallium cluster anions also appears related to both an approximate 1:1 atom:cluster charge in the polyanions and the strong relativistic effect for the element Tl.¹¹

The simultaneous occurrence of three or more anionic units in a single structure is rare because of the stringent conditions for a suitable combination of size factors and electronic requirements (closed shell covalent bonding, Madelung energy, and uniform Fermi energy). Some noteworthy examples are the closed-shell Ca₃₁Sn₂₀ (≡(Ca²⁺)₃₁(Sn⁴⁻)₅(Sn₂⁶⁻)₅(Sn₅¹²⁻))¹³ and Yb₃₆Sn₂₃ (≡(Yb²⁺)₃₆(Sn⁴⁻)₇(Sn₂⁶⁻)₅(Sn₆¹⁴⁻))¹⁴ in which isolated tin anions coexist with both dimers and larger linear oligomers. We report here a further example from cation size tuning that contains four different anionic units, namely, the nominal Tl⁵⁻, Tl₃⁷⁻, Tl₄⁸⁻, and Tl₅⁷⁻ in the phase Na₂₃K₉Tl_{15.3}. Correlations of the structure with the observed electrical and magnetic properties and Hückel MO calculations provide interesting implications regarding both multiple bonding in the striking Tl₃ trimer and possible delocalization of high lying (HOMO) electrons from highly charged anions, which are further conceptual extensions of Zintl compounds.^{6–8,14–16}

Experimental Section

Syntheses. All the syntheses were performed by reaction of the constituent elements. The surfaces of the Na chunks (99.9%, Alfa) and Tl metal bar (99.998%, Johnson-Matthey) were cleaned with a scalpel before use, while the K metal (99.9%, Baker) was used as received sealed under Ar. The general reaction techniques in welded Ta containers have been described elsewhere.⁹ Because both reagents and products are very sensitive to air and moisture, all operations were performed in a N₂- or He-filled glovebox with typical humidity levels less than 0.1 ppm (vol).

[⊗] Abstract published in *Advance ACS Abstracts*, May 1, 1996.

- (1) This research was supported by the Office of the Basic Energy Sciences, Materials Sciences Division, U.S. Department of Energy. Ames Laboratory is operated for DOE by Iowa State University under Contract No. W-7405-Eng-82.
- (2) Zintl, E. *Angew. Chem.* **1939**, 52, 1. Klemm, W.; Busmann, E. Z. *Anorg. Allg. Chem.* **1963**, 319, 297.
- (3) Schäfer, H. *Annu. Rev. Mater. Sci.* **1985**, 15, 1.
- (4) Corbett, J. D. *Chem. Rev.* **1985**, 85, 383.
- (5) Hughbanks, T. In *Inorganometallic Chemistry*, Fehlner, T., Ed.; Plenum Press: New York, 1992; p 291.
- (6) Nesper, R. *Prog. Solid State Chem.* **1990**, 20, 1.
- (7) Belin, C.; Tillard-Charbonnel, M. *Prog. Solid State Chem.* **1993**, 22, 59.
- (8) Corbett, J. D.; In *Chemistry, Structure and Bonding of Zintl Phases and Ions*, Kauzlarich, S., Ed.; VCH Publishers: New York, Chapter 4, to be published.
- (9) Dong, Z.-C.; Corbett, J. D. *Inorg. Chem.*, in press.

(10) Dong, Z.-C.; Corbett, J. D. *J. Am. Chem. Soc.* **1994**, 116, 3429.

(11) Dong, Z.-C.; Corbett, J. D. *J. Am. Chem. Soc.* **1995**, 117, 6447.

(12) Dong, Z.-C.; Corbett, J. D. *Angew. Chem. Int. Ed. Engl.*, in press.

(13) Ganguli, A. K.; Guloy, A. M.; Leon-Escamilla, E. A.; Corbett, J. D. *Inorg. Chem.* **1993**, 32, 4349.

(14) Leon-Escamilla, E. A.; Corbett, J. D. Unpublished research.

(15) von Schnering, H.-G. *Angew. Chem., Int. Ed. Engl.* **1981**, 20, 33.

(16) Miller, G. J. In *Chemistry, Structure and Bonding of Zintl Phases and Ions*; Kauzlarich, S., Ed.; VCH Publishers: New York; Chapter 5, to be published.

Table 1. Selected Data Collection and Refinement Parameters for Na₂₃K₉Tl_{15.3}

fw	4009
space group, <i>Z</i>	<i>P6₃/mmc</i> (No. 194), 2
lattice params, ^a Å	
<i>a</i>	11.235(1)
<i>c</i>	30.133(5)
<i>V</i> , Å ³	3294.0(8)
<i>d</i> _{calc} , g/cm ³	4.046
<i>μ</i> , cm ⁻¹ (Mo Kα)	384.4
residuals, <i>R</i> ; <i>R</i> _w ^b	0.049; 0.042

^a Guinier data, $\lambda = 1.540\ 562\ \text{\AA}$, 23 °C. ^b $R = \sum ||F_o| - |F_c|| / \sum |F_o|$; $R_w = [\sum w(|F_o| - |F_c|)^2 / \sum w(F_o)^2]^{1/2}$; $w = 1/\sigma^2$.

Different mixtures of Na, K, and Tl have been very productive in the isolation of novel thallium clusters.^{10–12,17} The title phase was first discovered from the product of a slowly cooled mixture of composition Na₁₃K₆Tl₁₀, which also yielded Na₁₅K₆Tl₁₈H¹⁷ (~40%) and another new ternary hexagonal compound (~10%).¹⁸ Once the stoichiometry had been established from crystallography, a pure phase of Na₂₃K₉Tl_{15.3} was obtained (according to Guinier powder data) from a stoichiometric mixture that was homogenized as a melt at 400 °C and annealed at 150 °C for 3 months followed by quenching of the container in ice water. Close-lying compositions such as Na₂₄K₉Tl₁₅ were indistinguishable in phase purity and showed no lattice constant shifts. Note that these quantitative synthesis features are powerful evidence for the assigned stoichiometry and against impurity stabilization, e.g., ~Cu in place of 1/3 Tl6 (below). The compound probably melts congruently around 300 °C because simple quenching of the melt without annealing also gave the title compound in high yield. The structure is not formed from Tl plus 23:9 mixtures of Na or K with Rb or Cs.

X-ray powder patterns for samples mounted between pieces of cellophane were collected with the aid of an Enraf-Nonius Guinier camera, Cu Kα radiation ($\lambda = 1.540\ 562\ \text{\AA}$), and NIST silicon as an internal standard. Least-square refinements of 67 lines indexed on the basis of the refined structural model resulted in the lattice constants given in Table 1.

Property Measurements. The resistivity of the pure phase was examined by a modified version of the electrodeless “Q”-meter method¹⁹ for a 102-mg sample that had been sieved to 250–400 μm and diluted with dried chromatographic Al₂O₃. Measurements were made at 34 MHz over the range 100–293 K. Magnetic susceptibility data were obtained from a 35-mg powdered sample held between two fused silica rods, which were in turn fixed inside silica tubing that was sealed at both ends under He. Measurements were made at a field of 3 T over the range of 6–300 K with the aid of a Quantum Design MPMS SQUID magnetometer. The raw data were corrected for the susceptibilities of the containers and the diamagnetism of the cores²⁰ as well as for the Larmor precession contribution of the delocalized valence electrons in the cluster orbitals, as before.^{10,21}

Structure Determination. A number of brittle blocklike crystals with black metallic luster were picked up from the product of a slowly cooled reaction, sealed in thin-walled capillaries, and then checked by Laue or oscillation photography for their singularity. A single crystal from the initial synthesis with dimensions ca. 0.12 × 0.13 × 0.10 mm was chosen for data collection, and this was carried out at 23 °C on a Rigaku AFC6R single crystal diffractometer with graphite-monochromated Mo Kα radiation. Programmed indexing of 25 reflections from a random search over $13 \leq 2\theta \leq 30^\circ$ yielded a hexagonal cell. Two octants of data were measured with 2θ up to 50° and then corrected for Lorentz and polarization effects and for strong absorption ($\mu = 384\ \text{cm}^{-1}$) with the aid of the average of six ψ -scan curves for strong reflections at different 2θ values. The assignment of the space group *P6₃/mmc* was made on the basis of the *6/mmm* Laue symmetry determined by the diffractometer, the systematic absences, and the

Table 2. Positional Coordinates and Isotropic Thermal Parameters for Na₂₃K₉Tl_{15.3}

atom	site symmetry	<i>x</i>	<i>y</i>	<i>z</i>	<i>B</i> _{eq} (Å ²) ^a
Tl1	<i>m</i>	−0.23598(6)	2 <i>x</i>	0.55511(6)	1.68(7)
Tl2	3 <i>m</i>	1/3	2/3	0.14360(9)	1.58(8)
Tl3	<i>m</i>	0.0973(1)	2 <i>x</i>	1/4	1.6(1)
Tl4	3 <i>m</i>	0	0	0.3362(1)	1.92(7)
Tl5	3 <i>m</i>	1/3	2/3	−0.1460(1)	2.9(1)
Tl6	6 <i>m</i> 2	1/3	2/3	3/4	3.6(6) ^b
K1	<i>m</i>	0.1319(5)	2 <i>x</i>	−0.0598(4)	3.6(5)
K2	<i>m</i>	0.4555(7)	2 <i>x</i>	1/4	3.8(8)
Na1	2/ <i>m</i>	1/2	0	0	3(1)
Na2	<i>m</i>	0.5040(8)	2 <i>x</i>	0.1164(5)	2.7(7)
Na3	<i>m</i>	0.1669(8)	2 <i>x</i>	−0.6540(6)	3.4(8)
Na4	3 <i>m</i>	1/3	2/3	−0.0396(9)	2.2(7)
Na5	<i>m</i>	0.1777(8)	2 <i>x</i>	−0.3103(5)	2.8(8)

^a $B_{eq} = (8\pi^2/3) \sum_i \sum_j U_{ij} a_i^* a_j^* \bar{a}_i \bar{a}_j$. ^b This position refined to be 31(2)% occupied.

Wilson statistics, and it was confirmed by the subsequent successful solution and refinement of the structure.

The structure was solved by direct methods.²² The first six apparent heavy atom positions were assigned to Tl atoms on the basis of both bond distances and peak heights, and subsequent least-squares refinements and difference Fourier syntheses quickly gave positions for all alkali-metal atoms. Refinements with isotropic thermal parameters proceeded smoothly except that the Tl6 atom on the fixed *2d* site (1/3, 2/3, 3/4; 6*m*2) exhibited an anomalously large thermal parameter. This suggested that the position was either fully occupied by a lighter element or partially occupied by Tl. However, assignment of Na to the position gave not only a very negative thermal parameter, or an occupancy of 230% ($B = 1.9\ \text{\AA}^2$), but also an unfavorable environment with two strongly bonded Tl5 atoms at 3.14 Å plus six Na neighbors at 3.53 Å, a very unreasonable distribution. A potassium occupancy was even less reasonable with very short Na–K and K–Tl separations and a 143% occupancy (2.3 Å²). These possibilities were thus excluded although such a model with 100% alkali metal on this site would not violate a closed-shell electron count for the compound (below). A multiplicity refinement for Tl at this site with all other atom occupancies fixed at unity and isotropic parameters gave a 30(2)% occupancy. Such a model is supported somewhat by the corresponding small elongation in the thermal parameter of the neighboring Tl5 along \bar{c} , and it is also consistent with the bonding and the electron counts addressed below. (The occupancy of the Tl6 at the (*2d*) site is presumably disordered as slow scans of all three axes on the diffractometer did not give any extra peaks, and the Guinier powder patterns and axial (Polaroid) photos did not show any superstructure lines.) Similar procedures applied to the occupancy refinements of Na, K, and all other Tl atoms (in parts) showed that these sites are fully occupied; the deviations from unity were all less than 3σ, and they were so fixed thereafter. The serious absorption effects, as illustrated by the large linear absorption coefficients (~384 cm⁻¹), were further corrected by DIFABS (as recommended)²³ after the isotropic refinement had converged (unnormalized transmission range of 0.82–1.29). The final anisotropic refinement, (576 independent reflections, 59 variables including a secondary extinction correction) converged with $R_w(F) = 4.2\%$, GOF = 1.34, and a partial occupancy of 31(2)% for the Tl6 position. The last corresponds to the formulation Na₂₃K₉Tl_{15.31(2)}. Complete refinement of a second data set collected from a crystal selected from a reaction run with a stoichiometry close to that refined gave the same results in all details. All data reduction and structure refinements were performed using the TEXSAN package²⁴ on a VAX station. A summary of some data collection and refinement parameters is listed in Table 1, the atomic positional and isotropic equivalent displacement parameters are in Table 2, and the important distances are given in Table 3. More details as well as anisotropic displacement parameters are contained in the

(17) Dong, Z.-C.; Corbett, J. D. *Inorg. Chem.* **1995**, *34*, 5709.

(18) Dong, Z.-C.; Corbett, J. D. Unpublished research.

(19) Shinar, J.; Dehner, B.; Beaudry, B. J.; Peterson, D. T. *Phys. Rev.* **1988**, *37B*, 2066.

(20) Selwood, P. W. *Magnetochemistry*, 2nd ed.; Interscience Publishers: New York, 1956; p 70.

(21) Sevov, S. C.; Corbett, J. D. *Inorg. Chem.*, **1992**, *31*, 1895.

(22) Sheldrick, G. M. SHELXS-86. Universität Göttingen, Germany, 1986.

(23) Walker, N.; Stuart, D. *Acta Crystallogr.* **1986**, *A39*, 158.

(24) TEXSAN, version 6.0; Molecular Structure Corp.: The Woodlands, TX, 1990.

Table 3. Bond Distances in Na₂₃K₉Tl_{15.3} (<4.5 Å)

Tl1–Tl1	2×	3.281(2)	Na1–Tl1	4×	3.274(1)
Tl1–Tl2		3.271(3)	Na1–K1	4×	4.052(7)
Tl1–K1	2×	3.989(2)	Na1–Na2	2×	3.51(1)
Tl1–K1		4.01(1)	Na1–Na4	2×	3.456(9)
Tl1–Na1	2×	3.274(1)			
Tl1–Na2	2×	3.43(1)	Na2–Tl1	2×	3.43(1)
Tl1–Na3		3.27(2)	Na2–Tl2		3.42(2)
Tl1–Na4		3.43(2)	Na2–Tl5		3.29(2)
			Na2–K1	2×	3.99(1)
Tl2–Tl1	3×	3.271(3)	Na2–K2		4.13(2)
Tl2–K2	3×	3.991(8)	Na2–Na1		3.51(1)
Tl2–Na2	3×	3.42(2)	Na2–Na3	2×	3.47(1)
Tl2–Na3	3×	3.25(1)	Na2–Na4		3.92(2)
			Na2–Na5	2×	3.81(2)
Tl3–Tl3	2×	3.280(4)			
Tl3–Tl4	2×	3.214(3)	Na3–Tl1		3.27(2)
Tl3–K2	2×	3.978(2)	Na3–Tl2		3.25(1)
Tl3–Na3	2×	3.20(2)	Na3–Tl3		3.20(2)
Tl3–Na5	4×	3.51(1)	Na3–Tl4		3.26(1)
			Na3–K1	2×	4.11(2)
Tl4–Tl3	3×	3.214(3)	Na3–K2	2×	4.10(2)
Tl4–K1	3×	4.05(1)	Na3–Na2	2×	3.47(1)
Tl4–Na3	3×	3.26(1)	Na3–Na5	2×	3.53(1)
Tl4–Na5	3×	3.54(2)			
			Na4–Tl1	3×	3.43(2)
Tl5–Tl6		3.135(4)	Na4–Tl5		3.20(3)
Tl5–Na2	3×	3.29(2)	Na4–K1	3×	3.97(1)
Tl5–Na4		3.20(3)	Na4–Na1	3×	3.456(9)
Tl5–Na5	3×	3.30(2)	Na4–Na2	3×	3.92(2)
Tl6–Tl5	2×	3.135(4)	Na5–Tl3	2×	3.51(1)
Tl6–K2	3×	4.11(1)	Na5–Tl4		3.54(2)
Tl6–Na5	6×	3.53(1)	Na5–Tl5		3.30(2)
			Na5–Tl6		3.53(1)
K1–Tl1		3.989(2)	Na5–K1		4.01(2)
K1–Tl1		4.01(1)	Na5–K2	2×	4.11(1)
K1–Tl4		4.05(1)	Na5–Na2	2×	3.81(2)
K1–K1	2×	4.45(2)	Na5–Na3	2×	3.53(1)
K1–K1	2×	4.43(2)	Na5–Na5		3.63(3)
K1–Na1	2×	4.052(7)			
K1–Na2	2×	3.99(1)			
K1–Na3	2×	4.11(2)			
K1–Na4		3.97(1)			
K1–Na5		4.01(2)			
K2–Tl2	2×	3.991(8)			
K2–Tl3	2×	3.978(2)			
K2–Tl6		4.11(1)			
K2–K2	2×	4.12(2)			
K2–Na2	2×	4.13(2)			
K2–Na3	4×	4.10(2)			
K2–Na5	4×	4.11(1)			

Supporting Information, and these as well as the structure factor data are available from J.D.C.

Results and Discussion

Anionic Substructure. The most remarkable features of this structure are, first, the simultaneous occurrence of four different “naked” thallium anions: Tl₅⁷⁻ (*D*_{3h}) as a regular trigonal bipyramid, Tl₄⁸⁻ (*C*_{3v}) as a slightly compressed tetrahedron, and Tl₃⁷⁻ as a linear trimer superimposed on Tl⁵⁻ as isolated atoms (Figure 1). The last two anions can be described as a randomly distributed 1:2 ratio of (Tl₃⁷⁻:Tl⁵⁻) arising from the one-third occupancy of the central Tl6 site. The formal charges (actually oxidation states) assigned to these anions correlate exactly with the closed shell configurations predicted from extended Hückel calculations (below). We will later return to the properties of the compound and whether these degrees of localization are reasonable. Analogous Tl₅⁷⁻ and Tl₄⁸⁻ polyanions have been previously identified, the former in Na₂K₂₁Tl₁₉¹⁰ as a distorted trigonal bipyramid with only mirror (*C*_s) symmetry through the

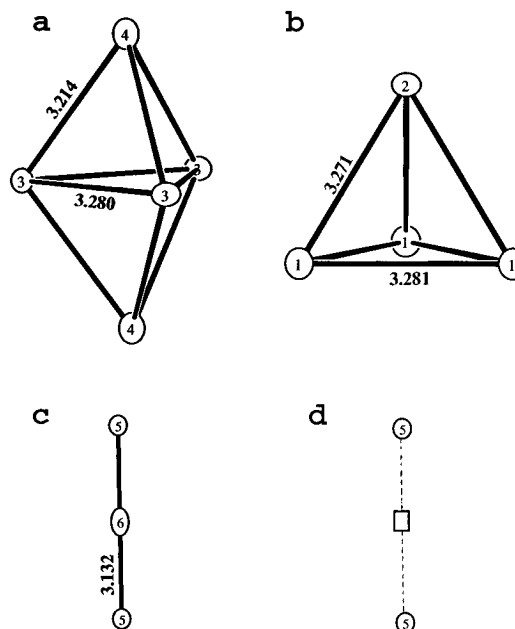


Figure 1. The isolated anions in Na₂₃K₉Tl_{15.3}: (a) trigonal bipyramidal Tl₅⁷⁻ (*D*_{3h}); (b) tetrahedral Tl₄⁸⁻ (*C*_{3v}); (c) linear trimeric Tl₃⁷⁻ (*D*_{∞h}); (d) the superimposed isolated Tl⁵⁻ where □ denotes the Tl6 vacancy (50% probability displacement parameters for all figures.)

waist atoms, and the latter in Na₂Tl²⁵ as a distorted tetrahedron (*C*₂). The geometries of both are closer to the ideals in the present structure according to the higher site symmetry imposed and the smaller span of edge lengths over each polyhedron, i.e., 3.21–3.28 Å vs 3.07–3.54 Å before for Tl₅⁷⁻ and 3.27–3.28 Å here vs 3.18–3.30 Å earlier for Tl₄⁸⁻. The average bond lengths over each polyhedron, 3.24 Å in Tl₅⁷⁻ and 3.28 Å in Tl₄⁸⁻, are consistent with the typical value of 3.25 Å observed in thallium anionic substructures, e.g., in NaTl²⁶ and A₈Tl₁₁ (A = K, Rb, Cs).²⁷

On the other hand, the linear Tl₃⁷⁻ trimer is the first homoatomic example among the boron group, although thallium dimers are found in Li₅Tl₂ (Tl–Tl = 3.01 Å)²⁸ and Sr₅Tl₃ (Cr₅B₃-type, Tl–Tl = 3.00 Å).^{14,29} (Electron-richer linear trimers Pn₃⁷⁻ with apparent 3c-4e bonding are well established in a variety of Ae₁₄MPn₁₁ phases, Ae = Ca–Ba, Pn = P–Bi.³⁰) An interesting trend in the dimensions of the polyanions is the noticeable increase of the (average) bond lengths from the dimer (~3.00 Å) to trimer (3.14 Å) and to deltahedra (~3.25 Å), which suggests multiple bonds *may* exist in the dimer and trimer (below). The linear Tl₃⁷⁻ trimer occurs when the Tl6 position is occupied, connecting the two neighboring Tl5 atoms, but when this position is vacant, the Tl5 atoms are unbonded and isolated Tl⁵⁻ ions. Isolated Tl anions are not new but have been observed in Na₆Tl,³¹ LiMg₂Tl,⁶ and Sr₅Tl₃.^{14,29} In practice, it is doubtful that the many highly charged anions defined in the present structure, Tl₅⁷⁻, Tl₄⁸⁻, Tl₃⁷⁻, and Tl⁵⁻, with charge: atom ratios ranging from –1.4 to –5.0, will exist in a localized sense unless they are well separated by solvating cations so that the higher energy electrons on anions are trapped or compensated by sufficient Coulomb interactions. In addition, polarization by the cations (covalency) will in real life reduce the actual

(25) Hansen, D. A.; Smith, J. F. *Acta Crystallogr.* **1967**, *22*, 836.

(26) Zintl, E.; Dullenkopf, W. *Z. Phys. Chem.* **1932**, *B16*, 195.

(27) Dong, Z.-C.; Corbett, J. D. *J. Cluster Sci.* **1995**, *6*, 187.

(28) Stöhr, J.; Schäfer, H. *Z. Naturforsch.* **1979**, *34B*, 653.

(29) Bruzzone, G.; Franceschi, E.; Merlo, F. *J. Less-Common Met.* **1978**, *60*, 59.

(30) Vaughney, J. T.; Corbett, J. D. *Chem. Mater.* **1996**, *8*, 671.

(31) Samson, S.; Hansen, D. A. *Acta Crystallogr.* **1972**, *28B*, 930.

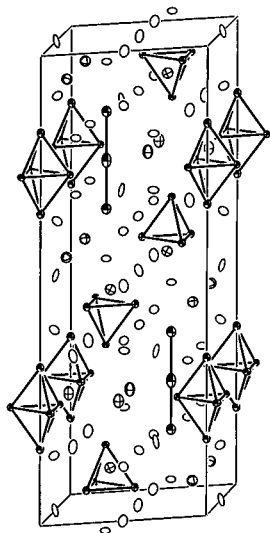


Figure 2. Approximate [100] view of $\text{Na}_{23}\text{K}_9\text{Tl}_{15.3}$ showing the distribution of isolated anions and alkali-metal cations within unit cell and the alternating stacking of Tl_5^{7-} layers with double Tl_4^{8-} layers along \bar{c} . The isolated Tl_3^{7-} feature cannot be seen because it overlaps with the trimer. Key: Tl, shaded; K, crossed; Na, open ellipsoids.

charges without having a significant effect on the Zintl picture. Important cation solvations are indeed always present, as illustrated by the present and all other alkali-metal–thallium compounds.^{8–11,27}

Cation Distributions and Anion Packing. Figure 2 shows the space partitioning of the isolated anions and the solvating cations in a unit cell. Each formula unit (half of a cell) contains one Tl_5^{7-} , two Tl_4^{8-} , one-third Tl_3^{7-} , and four-thirds Tl_1^{5-} , but the last feature cannot be seen in the plot because of disorder with the trimer. A 33% occupancy of the Tl6 atom is chosen here on the basis of both the refined value of 31(2)% ($\delta = 1\sigma$) and the closed-shell bonding that results (see below). Regardless of the differences in polyanionic identities and orientations, layers of Tl_5^{7-} stack alternately with double layers of Tl_4^{8-} along the c direction in an ABCACB (hcc)₂ sequence, still following close-packing principles.

The specific roles of cations about the cluster faces, edges, and vertices are to compensate anionic charges and to effectively separate (or bridge between) clusters. The cation distribution around the tetrahedral cluster is very similar to that found in Na_2Tl .²⁵ Each edge and face is bridged or capped by a Na atom, and all vertices have three exo-bonded K atoms (Figure 3a). However, the cation disposition about the trigonal bipyramid is different from that found for Tl_5^{7-} in $\text{Na}_2\text{K}_{21}\text{Tl}_{19}$ in which 20 cations (1 Na + 19 K) surround the polyanion in a quite anisotropic arrangement. The present Tl_5^{7-} ion is more tightly and uniformly sheathed by 24 cations (12 Na + 12 K), as shown in Figure 3b. All six triangular faces and six axial-to-equatorial edges are capped and bridged by a Na5 or Na3 atom, respectively, while three K1 atoms are exo-bonded to the more negative and open axial Tl4 and two K2 atoms are so bonded to the equatorial Tl3. Figure 3c shows the cylindrical cation arrangement around the Tl_3^{7-} trimer, with Tl5 within a slightly distorted cube and Tl6 in a pentacapped trigonal prism. One common feature in the cation distributions for all the anions is that the K atoms are involved only in relatively long exo functions leaving the smaller Na atoms to bridge or cap the polyhedral edges or faces.

Properties and Bonding. Magnetic susceptibility data for $\text{Na}_{23}\text{K}_9\text{Tl}_{15.3}$ as a function of temperature are shown in Figure 4. Diamagnetic corrections have been applied to exclude the contributions from the cores (-7.53×10^{-4} emu/mol) and the

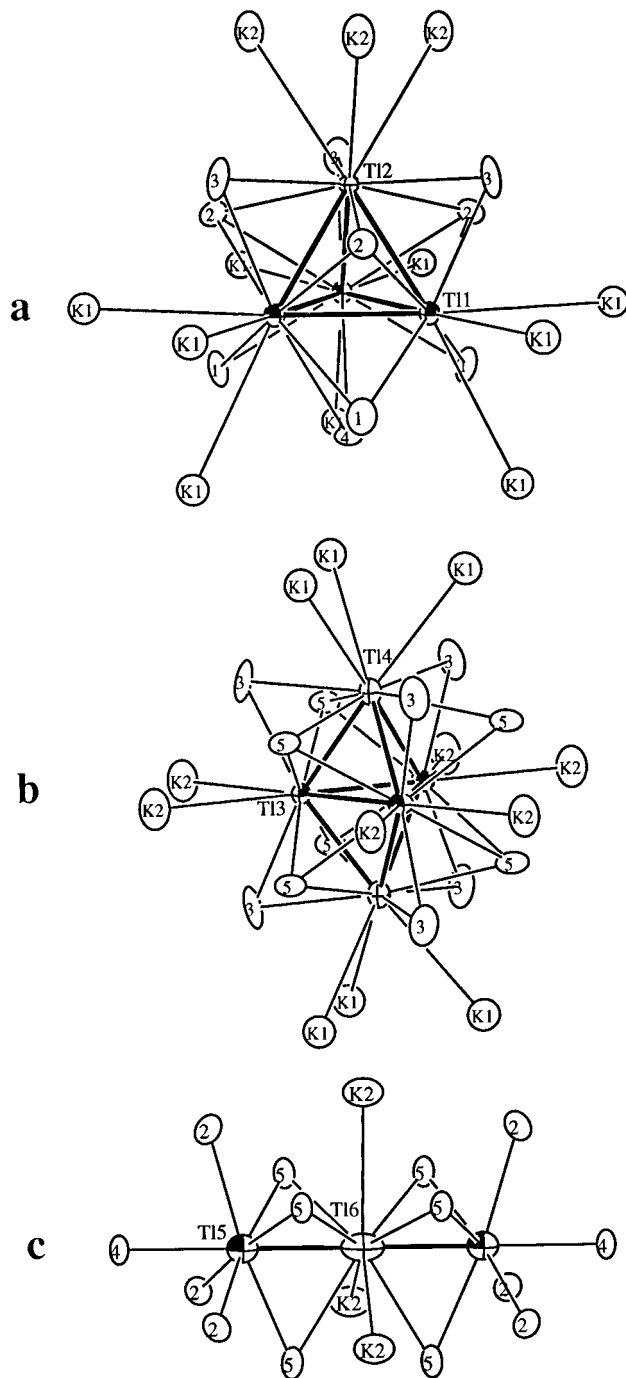


Figure 3. Cation dispositions around anions: (a) Tl_4^{8-} ; (b) Tl_5^{7-} ; (c) Tl_3^{7-} . Strong solvations are evident. (The numbered cations are all sodium.)

Larmor precession (-3.28×10^{-4} emu/mol) of the skeletal electrons in the isolated Tl_4^{8-} and Tl_5^{7-} clusters. The compound shows a substantially temperature-independent susceptibility over 6–300 K, a weak Pauli-paramagnetic property of $\sim 0.9 \times 10^{-3}$ emu/mol (or, to better reflect the large molar mass, 0.9×10^{-6} emu/cm³). A solid with a limited number of conduction electrons but essentially no localized unpaired spins in the structure is thus indicated. The temperature dependence of resistivity over 100–293 K in Figure 5 indicates a metallic behavior, $\rho_{293} \sim 90 \mu\Omega\cdot\text{cm}$ with a small temperature coefficient $\partial\rho/\partial T = +0.067(3)\% \text{ K}^{-1}$. These are common features of several alkali-metal compounds that contain larger thallium clusters; in fact the numbers are comparable to those found for $\text{Na}_3\text{K}_8\text{Tl}_{13}$.^{8,11,12}

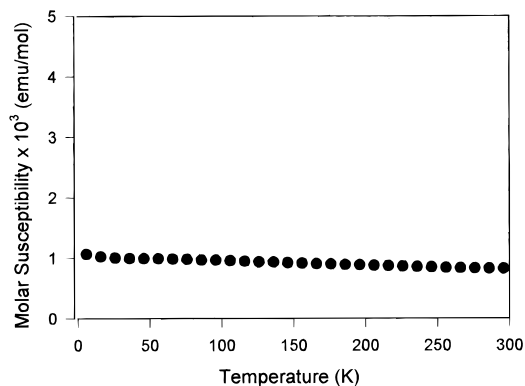


Figure 4. Temperature dependence of the molar susceptibility of Na₂₃K₉Tl_{15.3} over 6–300 K at 3 T.

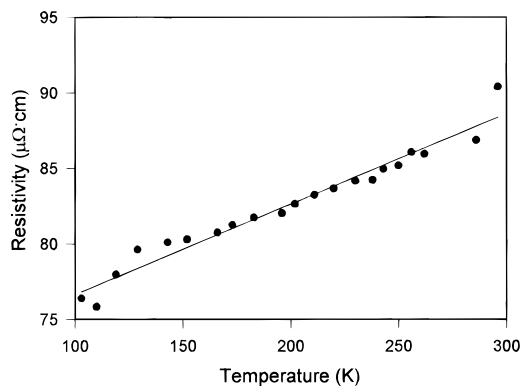


Figure 5. Resistivity of Na₂₃K₉Tl_{15.3} over 100–293 K by the “Q”-method.

However, it becomes a challenging task to understand the bonding of the anions and their apparent closed-shell configurations. Wade's rules (and extended Hückel calculations) easily predict an optimal 12 skeletal electrons for both a (closo) trigonal bipyramid and a (nido) tetrahedron, resulting in their formulations as Tl₅⁷⁻ and Tl₄⁸⁻ polyanions.³² The isolated thallium atom should require five more electrons to give an octet in a formal Tl⁵⁻ anion. Since each Na₂₃K₉Tl_{15.33} formula unit contains 32 alkali-metal atoms plus one Tl₅, two Tl₄, one-third Tl₃, and four-thirds isolated Tl units, complete electron transfer from alkali-metal atoms to the anionic substructure would give the remaining Tl₃ trimer a precise -7 charge [7×1 (Tl₅⁷⁻) + 8×2 (Tl₄⁸⁻) + $7 \times 1/3$ (Tl₃⁷⁻) + $5 \times 4/3$ (Tl⁵⁻) = 32].³³

Extended Hückel calculations on the observed trimer with the previously justified atomic parameters (Tl: 6s, $\zeta = 2.14$, $H_{ii} = -11.60$ eV; 6p, $\zeta = 2.04$, $H_{ii} = -5.80$ eV)¹⁰ in fact support such a configuration. The result is shown in Figure 6. Occupation of the first eight orbitals gives an optimal Tl₃⁷⁻ configuration with an essentially nonbonding HOMO ($1\pi_g^4$) at -5.80 eV and a HOMO-LUMO gap of ~0.94 eV. The penultimate bonding $1\pi_u^4$ orbital is followed by four more σ (s-p_z)-type orbitals, two bonding ($1\sigma_g$ and $2\sigma_u$) and two practically nonbonding.³⁴ It is interesting to see the relationship between the MO results and the coordination environment around Tl₃⁷⁻. The antibonding $2\sigma_g$ orbital consists mainly of an axial lone pair directed toward both of the close-lying Na4 atoms (3.20

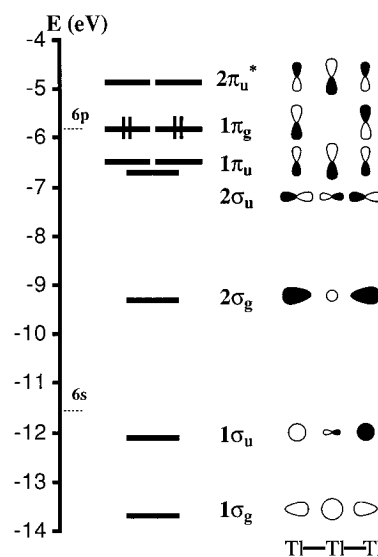


Figure 6. Extended Hückel orbital calculations for the observed thallium trimer. Diagrams on the right illustrate relative orbital populations (charges). The 6s and 6p ao energies are also marked.

Å), while the HOMO lone pairs (π_u^4 plus π_g^4) are polarized by cylindrical arrangements of Na₂, Na₅ and K₂ (Figure 3c). The 16-electron Tl₃⁷⁻ described in Figure 6 is, interestingly, isoelectronic and isosteric with CO₂. Significant differences with these heavy atoms and their parameters lie in the generation of an axial lone pair orbital in $2\sigma_g$ and, judging from the energy change, a significant $1\sigma_g$ bond from mainly 6s ao's, even though these are contracted. In addition, an energy decrease of -1.2 eV is calculated for the bonding $1\pi_u^4$ orbital, contrary to the general wisdom that the heavy elements are not effective at π bonding. The 3.13 Å Tl-Tl separations and the 6p orbital size are doubtlessly major factors in generating these results.

Whether the 3.14 Å Tl-Tl distance is indeed reasonable for a multiple bond is a little hard to establish independent of bonding considerations. Multiple bonds between elements from the third or higher periods are traditionally considered unstable because the larger atomic radii impede effective p π -p π overlap between neighboring atoms, and oligomerization or atomization becomes energetically more favorable.^{16,35} However, a number of exceptions have been found, not only in the organic compounds with Si=Si and P=P protected by sterically hindered groups, but also in lithium compounds that contain well-solvated tetrelide dimers Tt₂⁴⁻ (Tt = Si, Ge, Sn).^{6,36} A single bond might be taken as the 3.25 Å in NaTl, although this is close to the same values found in many clusters where there are fewer electron pairs than edges and the bonding is delocalized, so the NaTl lattice may be propped open a bit by the cation.⁹ The best that may be said is that the 3.13 Å bond length in Tl₃⁷⁻ is intermediate and not inconsistent with some degree of multiple bonding. The lower cation numbers around the Tl5 or Tl6 atoms in Tl₃⁷⁻ with respect to the other atoms in Tl₄⁸⁻ and Tl₅⁷⁻ are also consistent with the presence of multiple bonds.¹⁶ Certainly there are insufficient valence electrons according to the stoichiometry to allow only single bonds in the trimer even if all are localized, and the fractional content of Tl₃⁷⁻ seems more than an accident as it is precisely the amount to make the compound structurally closed shell.

The formation of multiply bonded dimers is insinuated by many Cr₅B₃-type structures as well. The Ae₅Tt₃ members are structurally all valence precise [(Ae²⁺)₅Tt₂⁶⁻Tt⁴⁻], the dimers

(32) Wade, K. *Adv. Inorg. Chem. Radiochem.* **1976**, *18*, 1.

(33) A whole alkali metal atom at the Tl6 site and only isolated Tl5 atoms also work out to a closed-shell count for 33 cations, namely, 7×1 (Tl₅⁷⁻) + 8×2 (Tl₄⁸⁻) + 5×2 (Tl⁵⁻) = 33. However, as pointed out in the text, such a model does not make sense either crystallographically or structurally.

(34) Further characterization is afforded by the orbital overlap populations for Tl₃⁷⁻: $1\sigma_g$, 0.527; $1\sigma_u$, 0.349 (with sizable energy differences); $2\sigma_g$, -0.080; $2\sigma_u$, 0.427; $1\pi_u$, 0.301 each, $1\pi_g$, 0.000.

(35) West, R. *Angew. Chem., Int. Ed. Engl.* **1987**, *26*, 1201.

(36) von Schnering, H.-G. *Angew. Chem., Int. Ed. Engl.* **1981**, *20*, 33.

being isoelectronic with F_2 , O_2^{2-} etc. However, oxidation of these also occurs to form interstitial hydrides or fluorides, and this shortens the Tl_2 bonds, evidently because π^* electrons have been removed in the formation of H^- or F^- . Ca_5Ga_3 and Sr_5Tl_3H are even more electron-deficient. The $Tl-Tl$ bond in the latter, 3.00 Å, is formally a triply bonded Tl_2^{4-} in the perhaps unlikely extreme that the other ion is really Tl^{5-} .¹⁴

The bonding energy gained through $p\pi-p\pi$ interactions in the present system is by no means comparable to that in organic compounds in free molecules, while, on the other hand, multiple bonding in this and related ionic phases in addition requires critical cation solvation around the anions (a favorable Coulomb trap) as well as efficient packing of cations and anions. The highest field Tl^{5-} has one more sodium neighbor than the remainder and has the greatest separation from thallium in other clusters. It is remarkable how the innate stabilities of a wide variety of thallium (and indium) clusters combine with rigorous requirements for anion bonding, cation solvation, and the packing of both in compounds to generate so many new compounds and novel structures that have, or are close to, closed-shell electronic configurations.

The observed metallic conductivity is conceptually contrary to the semiconducting properties expected for classical Zintl phases, although our explorations of the conduction characteristics for many phases have shown that this expectation is not always met. The present and other analogous Ga, In, and Tl compounds^{9-12,37-39} often show significant Pauli-like susceptibilities and even metal-like conduction characteristics, particularly with higher charged cations. Weak polarization (or covalent interactions) between anions and cations thus may result in time-averaged electron delocalizations within the network, perhaps via a semimetal-like band overlap, the highest lying filled cluster orbitals (bands) slightly overlapping those of the neighboring cluster and cation states indirectly or directly. However, these characteristics originate with the highest lying and most weakly bound electrons in the anion states or bands, and their properties should not be allowed to detract from obvious effects that more tightly bound states in covalent bonds have in generating clusters (or networks) with recognizable

closed-shell configurations. A great many classical Zintl phases have all the octet electrons on each atom tied up in covalent bonds. On the other hand, the situation with formal lone pairs in the higher charged clusters or monoatomic anions as well as those in analogous π^* states on the dimers and trimers cited is less certain. Some of these pairs may in fact fall above E_F and be delocalized or screened from the cores. Note that the loss of the π_g^4 electrons (Figure 6) would not alter the bonding in Tl_3^{7-} a bit. Band calculations on some of the Cr_5B_3 -type examples noted above support this notion for the π^* dimer states.¹⁴

The simultaneous occurrence of four different anions in the present structure demonstrates once again how delicately size factors and electronic requirements can combine to create unprecedented three-dimensional structures in which polyanions are trapped. These anions must respect a common Fermi energy (the individual HOMO-LUMO gaps must be consistent) so that the higher energy bound electrons need to be trapped by both anionic bonding and the Coulomb potentials. The presence of different-sized cations seems crucial for the formation of such multiple polyanion phases because of, first, the requirements to fill both small and large cavities in most structures and, second, the observation that no binary phases have been reported with such features. The critical role of the small Na atoms in the isolation of novel polyanions, as illustrated in $Na_2K_{21}Tl_{19}$,¹⁰ $Na_4A_6Tl_{13}$, and $Na_3K_8Tl_{13}$ ¹¹ and the present example, also suggests a promising cluster chemistry should result through mixing of the even smaller Li atoms. The absence of the present structure in mixed Na-(Rb, Cs) and K-(Rb, Cs) systems is probably related to size factors (e.g., Rb or Cs is too big to fill in the exo-bonded K positions). The present example together with other newly characterized phases¹⁰⁻¹² also suggests that there are a great many needs and opportunities left in the investigation of certain classes of Zintl phases. This is meant to include not only the electronics of bonding but also conduction and related properties.⁸

Acknowledgment. We thank J. Ostenson for the measurements of magnetic susceptibility data.

Supporting Information Available: Tables of crystallographic details and anisotropic displacement parameters (2 pages). Ordering information is given on any current masthead page.

(37) Henning, R.; Corbett, J. D. Unpublished research.

(38) Sevov, S. C.; Corbett, J. D. *J. Am. Chem. Soc.* **1993**, *115*, 9089.

(39) Sevov, S. C.; Corbett, J. D. *Inorg. Chem.* **1993**, *32*, 1059.